applied sciences

MDPI

Article

Assessment of the Sympathetic Detonation of Blasting Caps

Eugen Trană , Marin Lupoae *, Bogdan Iftimie and Alexandru Cătălin Casapu

Faculty of Integrated Armament Systems, Military Engineering and Mechatronics, Military Technical Academy "Ferdinand I", 050141 Bucharest, Romania
* Correspondence: marin.lupoae@mta.ro

Abstract: The neutralization of improvised explosive devices (IEDs) involves the use of disrupting agents propelled explosively. Due to the special nature of such materials, a proper investigation of the parts most susceptible to sympathetic detonation is in order. The initiation of IEDs is caused by detonation products, shock waves, and propelled disruptive agents. In this paper, initiation of IED composition (acceptor charge) due to the neutralization system's (donor charge's) explosive charge detonation is evaluated based on the influence of the first two of the three above-mentioned factors. One of the most susceptible components of IEDs to sympathetic initiation is the blasting cap. Based on an experimental and numerical mix approach, blasting cap tendency to sympathetic detonation in open field had been investigated. The suitability of critical energy fluence and Chapman–Jouguet threshold criteria to the sympathetic detonation tendency of blasting caps was investigated. Experimental and numerical/analytical results describing the phenomenon are in agreement.

Keywords: improvised explosive device; sympathetic detonation; blasting cap; numerical simulation

check for updates

Citation: Trană, E.; Lupoae, M.; Iftimie, B.; Casapu, A.C. Assessment of the Sympathetic Detonation of Blasting Caps. *Appl. Sci.* **2022**, *12*, 12761. https://doi.org/10.3390/app122412761

Academic Editors: Ricardo Castedo, Lina M. López and Anastasio P. Santos

Received: 4 November 2022
Accepted: 7 December 2022
Published: 12 December 2022

1. Introduction

Sympathetic detonation involves the initiation (usually unwanted) of an explosive charge called the acceptor due to the detonation of another charge called the donor. The initiation of the acceptor can be induced by detonation products and/or shock waves, depending on the distance between the two explosive charges.

The issue of sympathetic detonation is encountered in both military and civilian applications. In the military domain, avoiding sympathetic detonation is important, among other things, in the process of neutralizing IEDs or unexploded ordnance (UXO). In order to determine the critical distances at which the neutralization system can be placed, the possibility of sympathetic initiation of the IED load must also be taken into account since it is very important to avoid the effects that are produced by an unwanted initiation of the IED.

Starting from the principle of IED neutralization, namely preventing its operation (detonation of the explosive charge) and separating the component elements so that its functioning can no longer be triggered by the subsequent handling or interacting with the environment, the requirement of the neutralization system's performance can be formulated as the ability to induce a high enough shock in the IED to separate its parts, but at the same time to avoid the initiation of the explosive charge caused by the effects of the donor charge's detonation.

In both military and civilian fields, the storage, transportation, handling, and the production of explosives or items that include explosives involve risks due to the sensitivity and reactivity of such materials. As history has proven, one of the main risks is associated with the tendency of energetic materials to react to a nearby stimulus, such as an explosion or a kinetic impact. Over time, the above-mentioned tendency led to several catastrophic accidents in military facilities as well as in civil mining and industrial sites. Due to these tragic events, regulations regarding the design and use of items containing explosives were imposed. Among these regulations, sympathetic detonation evaluation tests are mandatory and can be seen as the backbone of safety program tests.

The evaluation of the tendency of an energetic material toward sympathetic detonation is assessed using the gap test. Basically, the gap test is a widely used test that aims to evaluate the sensitivity of explosives to blast waves. The gap test and other associated tests have been performed numerically and experimentally for different types of explosives, both on land and underwater, by several researchers throughout history. Thus, Yang et al. [1] numerically investigated Composition B's susceptibility to sympathetic detonation based on a Direct Numerical Simulation (DNS) scheme, which was also validated experimentally. They concluded that the probability of sympathetic detonation is related not only to the type of explosive and distance but also to the size of the charge. Zhang et al. [2] experimentally evaluated the underwater sympathetic detonation of TNT and analyzed the energy, pressure, and pulsing cycle. Kubota et al. [3,4] investigated using high-speed photography the sympathetic detonation of Composition B both in air and underwater and also investigated it numerically by using Lee and Tarver's phenomenological reaction-rate law. An experimental study by Becuwe and Delclos [5] on the sympathetic detonation of low-sensitivity explosive compounds (NTO and HMX-based PBX) showed that the shock insensitivity of the studied explosive mixture is combined with very good behavior under fire, slow heating, and a ball impact. Keshavarz et al. [6] studied the possibility of using a small-scale gap test to evaluate the sympathetic detonation of CaHbNcOd explosives and proposed a simple procedure for the analytical calculation of the shock sensitivity of energetic compounds. Ko et al. [7] investigated experimentally and numerically the shock sensitivity of a shaped charge underwater and showed that in an underwater explosion, the index of the sympathetic detonation is slightly higher than in the air. Along with the previously mentioned research teams, several others can easily be named, including researchers/teams that approached the subject in a theoretical manner, such as M.H. Keshavarz, E.N. Ferm, H.R. James, and A.C. Victor [6,8–10].

When an explosive charge (explosive bars) is subjected to the action of a shock wave, this shock wave will produce the initiation of the acceptor charge only if the energy of the shock wave is greater than the critical energy. The critical energy considers not only the pressure level (shock amplitude) but also the pulse duration and the acceptor impedance as stated by Walker and Wasley [11]. The formula for energy calculation is given in Equation (1).

$$E_c = P^2 t / \rho_0 U \tag{1}$$

where P is the shock amplitude, t indicates the pulse duration, ρ_0 denotes the acceptor's initial density, and U is the shock velocity that travels through the acceptor. The term E_c has the dimension of energy per unit area and is therefore referred to as energy fluence. Through experimental tests carried out with different explosives subjected to the square-wave shock produced by the impact of the flyer test, it was found that each explosive has a range of energy fluence in which a stable detonation is produced, called critical energy fluence [12]. Additionally, for the evaluation of the initiation of an explosive under the action of the shock wave, the "Pop-plot" [12] can be considered, which represents the graphic representation in logarithmic coordinates of the run distance as a function of pressure for the acceptor explosive.

The application of Equation (1) used to evaluate the initiation of detonation of an explosive charge requires the determination, by numerical analysis, of the amplitude and duration of the applied shock. In the absence of numerical analysis, the relationship developed by Yadav [13] takes into account detonation parameters, which are easier to measure and can be used to determine the energy transmitted to the explosive charge. This relation is specified in Equation (2).

$$E_c = \frac{\rho_0 D_j \delta \left[\frac{D_j - a_x}{2b_x} + \frac{D_j}{2(r+1)} \right]^2}{D_j - \left[\frac{D_j - a_x}{2b_x} + \frac{D_j}{2(r+1)} \right]} \quad (2)$$

where ρ_0 is the initial density, D_j is the velocity of detonation, δ is the thickness of reaction, r denotes the specific heat ratio of detonation products, and a_x and b_x are Hugoniot constants.

In line with the sympathetic detonation issue, yet in a less conventional manner, the current paper focuses on the investigation of the sympathetic detonation tendency of the blasting cap, containing pentaerythritol tetranitrate (PETN) charges. The main focus is targeted on investigating the applicability of critical energy fluence for a particular configuration with an air gap between donor and acceptor explosive charges.

For the assessment of the detonation initiation potential of a blasting cap, in this paper, we will use Equation (1) because, when using numerical analysis, the parameters in this equation are determined much faster. The relevance of the study is obvious when one considers the specific way in which the neutralization of suspicious packages is carried out. Basically, the disruption of such packages is performed by propelling a disrupting agent (metallic/plastic bolts or water) with the use of small explosive charges. The blast wave generated by the detonation of an explosive charge has the potential, in certain conditions, to lead to unwanted package detonation due to the initiation of explosive charge and/or blasting caps.

2. Experimental Investigation

In order to experimentally evaluate the sensitivity of blasting caps to blast waves, several tests have been performed. The experiments involved the use of 100 g of TNT as donor charge and ϕ7 × 69 mm blasting cap as an acceptor. TNT was chosen as a donor because it is considered a reference explosive. Although the amount of 100 g of explosive is not common for neutralization systems, it was used to better capture the influence that the detonation products and the shock wave can have on the sympathetic detonation of a blast initiator. The experimental setup illustrated in Figure 1 aims to identify a critical distance, in terms of air thickness, between the acceptor and the donor that will end in a no-go reaction for the acceptor.

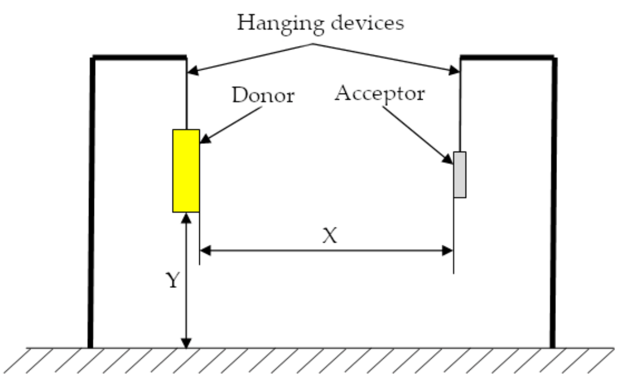

Figure 1. Experimental set-up (side-on configuration).

The blasting cap type used in these experiments is based on 0.6 g PETN charge with a density of 1.75 gm/cm^3. The donor charge was detonated using the same type of blasting cap as the detonator as the one used as the acceptor.

The tests were performed in an open space configuration, imposing a higher y value (donor/ground distance) than the x value (donor/acceptor distance). Using this approach, the incident blast wave was allowed to arrive first at the acceptor position instead of a one reflected. The post-test recovery of target blasting caps, when possible, was the criterion for identifying a possible detonation of the acceptor. A witness plate was not used due to the chosen test setup (the TNT charge was parallel to the blasting caps in order to have a larger contact surface; this represents the most unfavorable situation in relation to the position that a disruption load can have towards an acceptor load from the components of an IED). In this situation, the presence of a witness plate could have influenced the initiation of the blast cap from the shock wave that is reflected from the plate.

Table 1 lists the experimental results regarding blasting cap sympathetic detonation tendency.

Table 1. Gap test experimental results.

Air Gap Thickness X (mm)	Go/No Go
100	Go
200	Go
350	No go
500	No go

A fast image recording camera (Photron, FASTCAM SA-Z), set to an acquisition rate of 30,000 fps, was used as part of the testing setup. Thus, the blast wave position and fireball dimension during experimental tests were traced. Table 2 contains the results that were extracted from image analysis, and the detonation of 100 g TNT is illustrated in Figure 2.

Table 2. Blast wave position and fireball dimension.

Time (s)	Blast Wave Position (mm)	Fireball Dimension (mm)
0	0	0
0.0003000	608.39	623.04
0.0005330	715.52	798.26
0.0006670	749.59	900.48
0.0009670	827.45	1061.09
0.0016330	851.79	1406.67
0.0036670	992.94	1596.58
0.0050330	1017.28	N/A
0.0067670	1065.96	N/A
0.0114330	1168.17	N/A

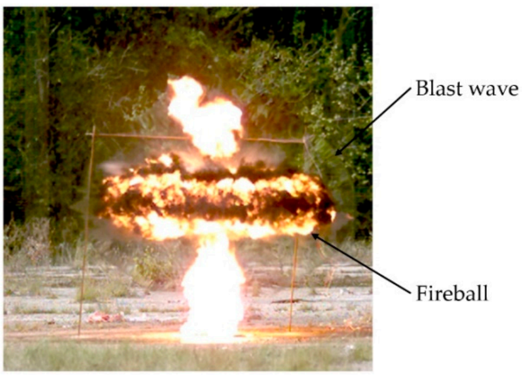

Figure 2. Typical image of 100 g TNT detonation.

3. Numerical Approach

While experimental testing is the most suitable method to evaluate sympathetic detonation, the numerical approach has proved to be a valuable tool in deciphering the process specifics. Thus, important aspects of the detonation propagation process (pressure level in the donor/acceptor charge or run distance for a stable detonation) can be investigated using a low-cost and reasonable-time scenario. For the proposed experimental tests, numerical models have been defined using Autodyn 2021® software [14].

3.1. Preprocessing

In order to corroborate the experimental results with the numerical ones, one simple approach was considered. The numerical model is based on a 2D planar symmetrical geometry and the use of multi-material Euler part.

Since the mesh sensitivity is a well-known characteristic of commercial software based on the Finite Element Method (FEM), special attention was given to this aspect. Considering Ko's observation [7] regarding the recommended mesh dimension as a function of the distance for the free air blast wave and also the distances involved in experimental tests, a graded mesh was imposed. The mesh dimension varies in both directions from 0.1 mm in the blasting cap region to 1 mm in the donor charge area, as shown in Figure 3.

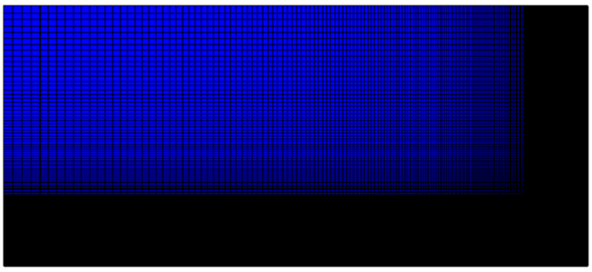

Figure 3. Typical mesh example.

In addition to the above-mentioned aspects, it must be pointed out that two rows of six gauges, 1 mm apart on the X axis and 5 mm apart on the Y axis, were used for numerical calculus to record the peak pressure in the acceptor charge. The position of the gauges, the material location, and the edges on which boundary condition were imposed, as shown in Figure 4. Additionally, in order to reduce the simulation time, the pressure contours generated by 100 g TNT detonation have been remapped in the current simulation using the fill option from a separate Autodyn 2021® file.

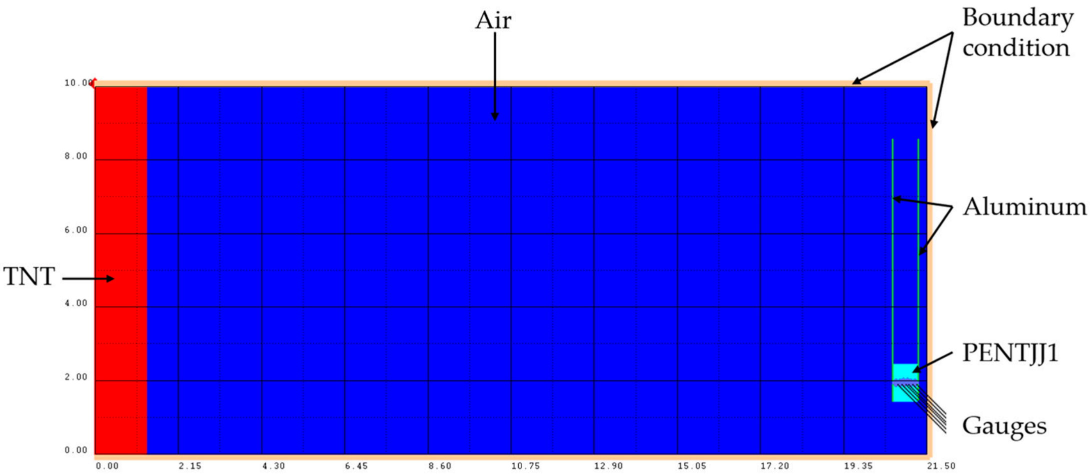

Figure 4. Materials location and gauges position.

3.2. Material Models

The basic properties of any substance, explosives included, are usually identified through a mathematical relation that correlates pressure, volume, and internal energy/ temperature. The relation is called an equation of state (EOS).

In the process of numerical analysis of the sympathetic detonation, it was found that the choice of the equation of state that describes the behavior of the donor and acceptor charges plays a very important role.

Over time, numerous attempts to define an EOS that accurately predicts the behavior of explosive gas products have been made. In fact, the number of proposed equations was high enough to classify them into two distinct categories: one considers the chemistry explicitly and the other does not [15].

Unfortunately, all of the above-mentioned equations have limited the applicability and variable accuracy. Despite this shortcut, their use in numerical calculus is extremely beneficial since different particular situations can be investigated in a reasonable time frame and an almost costless manner.

When explosive detonation applications are numerically investigated, one EOS is usually involved, namely Jones–Wilkins–Lee (JWL) [16]. In fact, the use of the JWL EOS is so common that by now almost all hydrocodes have implemented it and several forms can be identified in the literature. However, the most known form of equation is the form of a family of isentropes [17], which is illustrated in Equation (3).

$$p(S, V) = Ae^{-R_1 V} + Be^{-R_2 V} + C^*(S)V^{-(\omega+1)} \tag{3}$$

where p is the pressure; S refers to the entropy per unit initial volume (s/v_0); V is the volume relative to the undetonated state (v/v_0); A, B, R_1, and R_2 are constant fitting parameters; ω is an assumed-constant material parameter (Grüneisen function); and $C^*(S)$ is a parameter dependent only upon the entropy S.

Based on the previously mentioned JWL EOS and ideal gas EOS assumptions, the pressure in the front of a traveling blast wave can be accurately evaluated when hydrodynamic simulations are employed. Even though the equation's versatility is impressive, the application of JWL EOS by itself cannot deliver crucial data regarding the initiation of the explosive when subjected to blast wave stimulus. Thus, in order to investigate the blasting cap sympathetic detonation susceptibility, a slightly different EOS was chosen, the Lee–Tarver equation of state [18]. In fact, the Lee–Tarver EOS is basically a JWL EOS that has been upgraded with a supplementary equation, Equation (4), that allows the evaluation of the burning fraction based on the pressure level acting on/inside the explosive [18].

$$\frac{\partial F}{\partial t} = I(1-F)^b\left(\frac{\rho}{\rho_0} - 1 - a\right)^x + G_1(1-F)^c F^d p^y + G_2(1-F)^e F^g p^z \tag{4}$$

where F is the explosive burning fraction which has a value between 0 and 1.

The importance of JWL EOS and Lee–Tarver EOS for the current blast cap sympathetic detonation study is correlated with the Chapman–Jouguet pressure level that can be used as the Go/No-Go criterion.

The materials used in the numerical simulation are TNT for the donor charge, PETNJJ1 for the acceptor charge, aluminum for the blasting cap walls, and air for the space between the donor and the acceptor. All the equations of state (EOS) and strength models of the materials were adopted from the library of the Autodyn 2021® software.

3.3. Numerical Results

The obtained numerical results are presented in Table 3. In Figure 5, the pressure levels recorded by two different gauges located inside the acceptor charge are illustrated for two cases. Figure 5a shows the pressure levels in the case of a 200 mm gap between the donor and acceptor, while Figure 5b shows the results for a distance of 500 mm. The peak overpressure was directly measured from the gauges. The pressure wave speed was determined from graphs of pressure in time, for consecutive sensors. By dividing the distance between the sensors by the values of the times at which the maximum values of the pressures were obtained, the shock wave velocities were determined for each case of the acceptor–donor charge. The critical energy fluence was determined by using the maximum pressure value, speed, and the pulse duration of the shock wave. For the calculation of the shock wave pulse duration, the area under the pressure–time curve was numerically evaluated and then approximated with a square-shaped pulse (rectangle with a height given by the maximum pressure value and length given by the value of pressure-acting time that equals the previously calculated impulse).

Table 3. Virtually measured data in acceptor charge.

Air Gap Thickness, X (mm)	Peak Overpressure (Mbar)	Pressure Wave Speed (mm/ms)	Critical Energy Fluence (J/m^2)
100	4.02×10^{-3}	3162	1.69×10^5
200	3.55×10^{-3}	2881	1.51×10^5
350	1.58×10^{-5}	2840	97.38
500	0.91×10^{-5}	2739	37.46

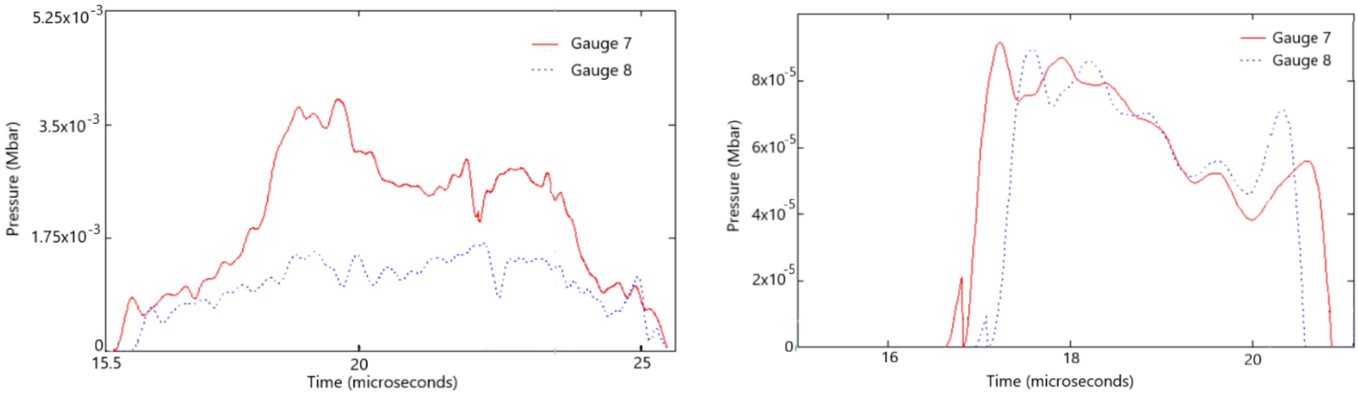

(**a**) 200 mm case (**b**) 500 mm case

Figure 5. Typical examples of numerically recorded pressure history in PETNJJ1 material (gauges 7 and 8 are the first and second gauges from the upper row).

4. Discussion

As the main goal of the present study is to evaluate the sympathetic detonation tendency of blasting caps, the main focus is on the correlation of experimental and numerical results.

If the experimental approach is a straight forward method that clearly points out the presence of acceptor detonation, the numerical approach is somehow trickier.

As previously mentioned, the numerical simulation is based on the use of Lee–Tarver EOS [19]. The Lee–Tarver EOS points mainly at the Chapman–Jouguet [19,20] findings that were later included in von Neumann's work [21]. Basically, a stable detonation is achieved when the pressure level reaches a certain value that is specific to each explosive (0.327 Mbar for PETN). Considering this approach, the blasting cap will not be susceptible to sympathetic detonation (in a range of a 0.1 to 0.5 m clearance distance) as long as the pressure recorded by the gauges indicates significantly lower levels (see Table 3). Nevertheless, as experimental tests have proved, the blasting cap detonation manifested at both 100 mm and 200 mm, where, according to numerical simulation, the peak overpressure is less than 0.327 Mbar.

Acknowledging the hypothesis involved in the critical energy fluence theory (step pulse shape and constant impedance, mainly) and the 1.5×10^5 J/m^2 threshold value for the energy fluence of PETN (1.75 gm/cm^3) [22], the calculus based on the numerical data (Figure 5) indicates a very good match with the experimental observation (see Tables 1 and 3). Thus, it is found that for distances of 100 mm and 200 mm, the critical energy values are close to the threshold value for the initiation of the acceptor explosive. On the other hand, the recorded pressures are lower than those corresponding to the C-J state, which indicates a weak detonation. The values of the maximum pressure and the duration of the positive phase of the phenomenon shown in Figure 5a fall within the values presented in the literature for the initiation of solid explosives [23]. Moreover, the shape of the pressure–time curve in Figure 5a is similar to the ones in Walker and Wasley's work [24] at the point that the initiation of the explosive occurs. Additionally, by analyzing Figure 5, it can be observed that the pressure wave shape acting on the blasting cap has a much different profile from the ones usually recorded during a standard gap test.

Due to the mismatch between the shock wave's front velocity and donor gas products' front velocity, the first to act on the blast cap is the blast wave, and the gas products pressure shortly afterward, depending on the relative position between the donor and acceptor charges, as can be deduced from Figure 6. The pressure wave profile is also shaped by the reflected blast wave, which is clearly indicated by the numerical simulation.

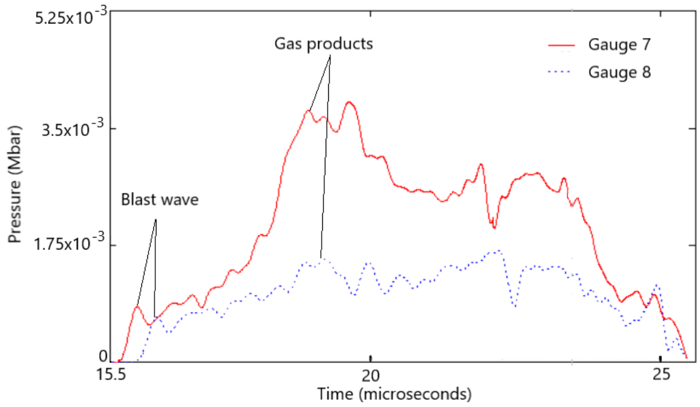

Figure 6. Pressure wave profile (200 mm case).

The same outcome can be underlined by theoretical means as well. Therefore, using far-field experimental data (images recorded when the blast wave has already traveled over a 0.6 m distance), the Sedov-Taylor model [25,26], and Gilev's observations [27], one can predict the distance between the incident blast wave and the gas products' border. Useful data regarding the position of the blast wave and the gas products' border can be extracted by solving Equations (5)–(10) [25–29]. In Figure 7, a comparison between experimental results and the application of Equations (5)–(10) for two values of the expansion dimensionality factor is presented.

$$R_s(t) = at^b \tag{5}$$

$$a = \left[\frac{E_d/(\tau_0^s l_0^{3-n})}{\rho}\right]^{1/(n+2)} \tag{6}$$

$$b = \frac{s+2}{n+2} \tag{7}$$

$$l_0 = \left(\frac{3m}{2\pi\rho}\right)^{1/3} \tag{8}$$

$$\tau_0 = \frac{l_0}{v_{TNT}} \tag{9}$$

$$R_f(t) = R_{max}\left(1 - e^{-kt}\right) \tag{10}$$

where $R_s(t)$ indicates the shock front radii; a and b are coefficients; E_d is the TNT release energy during detonation (usually 4.1 MJ/kg); l_0 denotes a length scale; τ_0 denotes a time scale; m is the TNT mass; ρ is the TNT mass density; v_{TNT} denotes the TNT detonation velocity (6940 m/s); s indicates a factor characterizing the rate of energy release: instantaneous energy release (s = 0) and constant-rate energy release (s = 1); n is the expansion dimensionality: planar expansion (n = 1), cylindrical expansion (n = 2), and spherical expansion (n = 3); $R_f(t)$ indicates the fireball radii; R_{max} is the fireball stopping radii (0); and k denotes the drag coefficient.

It must be stated that the Sedov–Taylor equation can be applied only to the mid-field region according to Equation (11) [28].

$$\left(\frac{3m}{2\pi\rho}\right)^{1/3} \ll R_s \ll \left(\frac{\Delta H_d}{p}\right)^{1/3} \tag{11}$$

where ΔH_d indicates the total energy released during detonation, afterburning included, (up to 10.1 MJ/kg [30]), and p denotes the ambient pressure.

Using high-speed camera imaging, R_s radii can be identified for different time values. Since the TNT charge has a cylindrical shape, a factor n = 2 was considered. Additionally, due to the fact that the distances between the TNT charge and the blasting cap are small (less than 0.5 m) for the experimental setup, an instantaneous energy release (s = 0) was set. However, the experimental results plotted against the results provided by Equation (5), which are presented in Figure 7a, show some considerable differences.

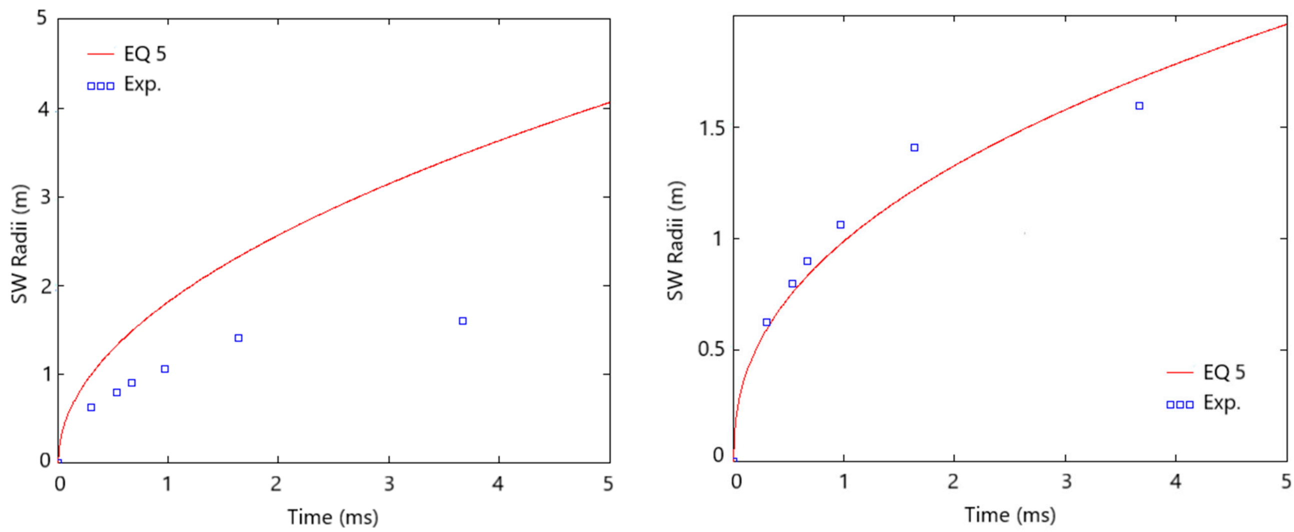

(**a**) n = 2 (**b**) n = 2.7

Figure 7. Experimental vs. Equation (5) results.

By closely analyzing the footage in Figure 8, it can be observed that the blast wave shape presents itself neither as a cylindrical shape nor as a spherical one. The mismatch is probably due to the ratio between the length and the diameter of the TNT blast charge, which has a value of 3.57, and also due to the overall small dimensions of the charge. Considering the experimental blast's wave shape, which is more like an ellipsoid, a different value for n factor was chosen, namely 2.7. A comparison between predicted and experimental results for the modified value of the n factor is presented in Figure 7b, and it is clear that the use of this value leads to a much better approximation of the experimental data.

The R_f radii can also be calibrated with the use of the camera footage and finally plotted against R_s values, as shown in Figure 9. Predictions using Equation (11) are plotted in the same figure. With the use of Figure 9, one can easily see that the blast wave gradually moves away from the fireball border, which is consistent with the data provided by the numerical simulation.

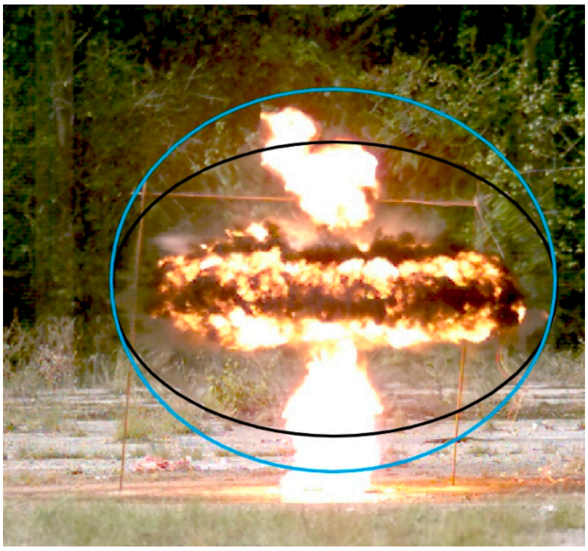

Figure 8. Blast wave shape (perfect sphere (blue) and real (black)).

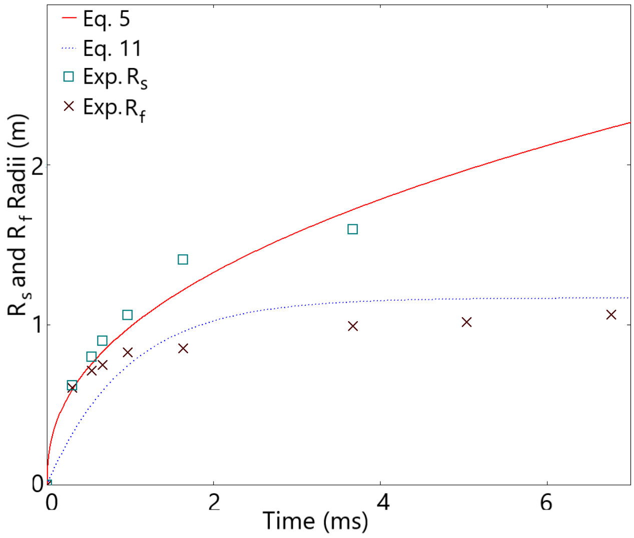

Figure 9. Blast wave vs. Fireball Radii.

The analytical calculus based on Equations (5)–(10) is confirmed by a numerical approach, as shown in Figure 10. According to Figure 10, the blast wave front gradually speeds up, leaving behind the front of the donor gas products.

As mentioned in Section 3.1, two rows of gauges (six gauges/row) were used for pressure recording in the acceptor charge. This particular choice was due to the close distance between the donor and acceptor charges which resulted in a curved shock wave front, as depicted in Figure 10. As a result of the curved shock wave front, the first susceptible area to interact with the blast wave is the upper front of the acceptor charge. This can be clearly seen in Figure 5, where the higher-pressure values are recorded by gauges no. 7 and 8.

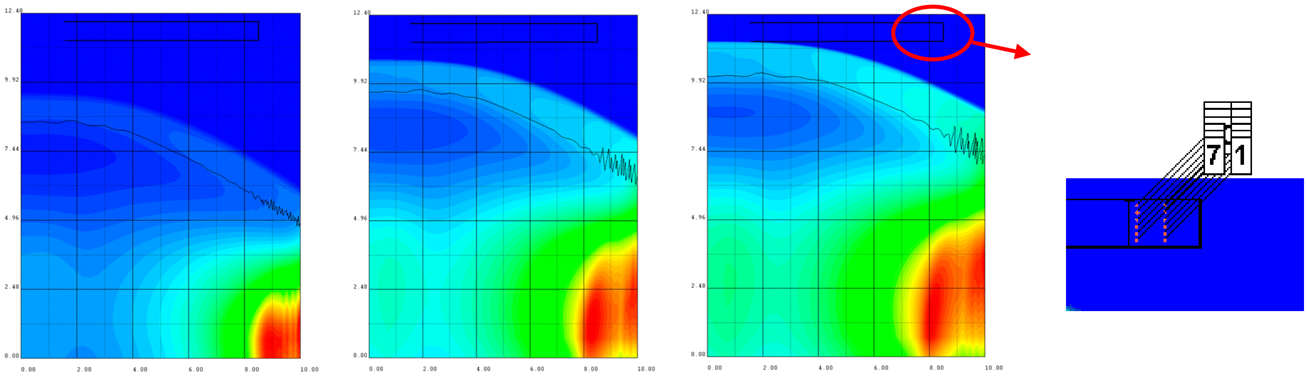

(**a**) t = 2 µs (**b**) t = 6 µs (**c**) t = 8 µs (**d**) Gauges placement

Figure 10. Blast wave front vs. TNT gas products front for 100 mm air gap thickness case.

5. Conclusions

Sympathetic detonation tendency of the blasting cap for different scenarios is mandatory when the disrupting equipment is used on suspicious packages (IEDs). While experimental tests easily allow the evaluation of blasting cap sensitivity to blast waves, the mix between numerical and experimental approaches can enhance the understanding of the phenomenon.

Based on the relations of the mathematical model, it can be concluded that the shock wave detaches gradually from the donor gas products, the complete detachment being completed at a greater distance than the ones characterized by the blast cap initiation. In the nearby distance of the donor charge, both the shock waves' and the gas products' overpressure act on and initiate the blasting caps, even though not simultaneously, as proved in Figure 6. It is also clearly pointed out that the presence of gas products favors reaching the critical value for sympathetic detonation, according to the critical energy fluence criterion.

The analysis of sympathetic detonation tendency of blasting caps in close vicinity shows that the critical energy fluence criterion is preferable to the Chapman–Jouguet pressure threshold. The critical energy fluence criterion can be applied to test configurations that include not only a dense matter gap but also an air gap.

Author Contributions: Conceptualization, M.L. and E.T.; methodology, E.T. and M.L.; software, E.T and A.C.C.; validation, E.T., M.L. and A.C.C.; formal analysis, E.T., M.L. and B.I.; investigation, M.L., B.I., E.T. and A.C.C.; resources, M.L. and B.I.; data curation, E.T.; writing—original draft preparation, E.T. and B.I.; writing—review and editing, M.L., E.T. and A.C.C.; visualization, E.T., B.I. and A.C.C.; supervision, E.T.; project administration, M.L.; funding acquisition, M.L. All authors have read and agreed to the published version of the manuscript.

Funding: The paper was partially supported by a grant of the Romanian Ministry of Innovation and Research, UEFISCDI, project number 33SOL/2021 within PNCDI III.

Institutional Review Board Statement: Not applicable.

Informed Consent Statement: Not applicable.

Data Availability Statement: Not applicable.

Conflicts of Interest: The authors declare no conflict of interest.

References

1. Yang, T.; Wang, C.; Li, T. Numerical simulation study of sympathetic detonation in stages. *Def. Technol.* **2021**, *18*, 1382–1393. [CrossRef]
2. Zhang, Z.; Wang, C.; Hu, H.; Yang, T. Investigation of underwater sympathetic detonation. *Prop. Explos. Pyrotech.* **2020**, *45*, 1736–1744. [CrossRef]

3. Kubota, S.; Shimada, H.; Matsui, K.; Liu, Z.-Y.; Itoh, S. High-speed photography of underwater sympathetic detonation of high explosives. In Proceedings of the 24th International Congress on High-Speed Photography and Photonics, Sendai, Japan, 24–29 September 2000; Volume 4183, pp. 763–770.
4. Kubota, S.; Liu, Z.Y.; Otsuki, M.; Nakayama, Y.; Ogata, Y.; Yoshida, M. A Numerical study of sympathetic detonation in gap test. *Mater. Sci. Forum* **2004**, *465–466*, 163–168. [CrossRef]
5. Becuwe, A.; Delclos, A. Low-sensitivity explosive compounds for low vulnerability warheads. *Prop. Explos. Pyrotech.* **1993**, *18*, 1–10. [CrossRef]
6. Keshavarz, M.H.; Motamedoshariati, H.; Pouretedal, H.R.; Tehrani, M.K.; Semnani, A. Prediction of shock sensitivity of explosives based on small-scale gap test. *J. Hazard. Mater.* **2007**, *145*, 109–112. [CrossRef] [PubMed]
7. Ko, Y.-H.; Kim, S.-J.; Yang, H.-S. Assessment for the sympathetic detonation characteristics of underwater shaped charge. *Geosystem Eng.* **2017**, *20*, 286–293. [CrossRef]
8. Ferm, E.N.; Ramsay, J.B. Spherical projectile impact on explosives. In Proceedings of the Ninth Symposium (International) on Detonation, Portland, OR, USA, 28 August–1 September 1989; Volume 2, pp. 1427–1431.
9. James, H.R. Critical energy criterion for the shock initiation of explosives by projectile impact. *Prop. Explos. Pyrotech.* **1988**, *13*, 35–41. [CrossRef]
10. Victor, A.C. A Simple method for calculating sympathetic detonation of cylindrical, cased explosive charges. *Prop. Explos. Pyrotech.* **1996**, *21*, 90–99. [CrossRef]
11. Walker, F.E. A Comparison of the Classical and a Modern Theory of Detonation. *J. Phys. IV Proc.* **1995**, *5*, C4-231–C4-257.
12. Cooper, P.W. *Explosives Engineering*; Wiley: New York, NY, USA, 1996.
13. Yadav, H.S.; Asthana, S.N.; Subhananda, A. Critical Shock Energy and Shock and Detonation Parameters of an Explosive. *Def. Sci. J.* **2009**, *59*, 436–440. [CrossRef]
14. ANSYS Inc. *AUTODYN User Manual*, version 14.0; ANSYS Inc.: Beijing, China, 2013.
15. Fickett, W.; Davis, W.C. *Detonation: Theory and Experiment*; Dover Publications: Mineola, NY, USA, 2011; p. 25.
16. Kubota, S.; Saburi, T.; Nagayama, K. Unified Form EOS for Detonation Products Based on Relationship between Initial Density and Detonation Velocity. *AIP Conf. Proc.* **2020**, *2272*, 030012.
17. Seglets, S.B. *An Examination of the JWL Equation of State*; ARL-TR-8403; US Army Research Laboratory: Adelphi, MD, USA, 2018.
18. McIntosh, G.W.J. *Explosive Modelling Using Ls-Dyna—A User Guide*; Technical Memorandum; Defence R&D Canada: Valcartier, QC, Canada, 2014.
19. Chapman, D.L. VI. On the rate of explosion in gases. *Philos. Mag.* **1899**, *47*, 90–104. [CrossRef]
20. Jouguet, E. Sur la propagation des réactions chimiques dans les gaz. *J. Math. Pures Appl.* **1905**, *1*, 347–425.
21. Von Neumann, J. Theory of detonation waves. In *Collected Works*; Taub, A.H., Ed.; Pergamon Press Ltd.: Oxford, UK, 1963; Volume 6, pp. 178–218.
22. Schwarz, A.C. *New Technique for Characterizing an Explosive for Shock Initiation Sensitivity*; SAND75-0314 Report; Sandia Labs.: Albuquerque, NM, USA, 1975.
23. Walker, F.E.; Wasley, R.J. A general model for the shock initiation of explosives. *Prop. Explos. Pyrotech.* **1976**, *1*, 73–78. [CrossRef]
24. Walker, F.E.; Wasley, R.J. Initiation of nitromethane with relatively long-duration, low-amplitude shock waves. *Combust. Flame* **1970**, *15*, 233–246. [CrossRef]
25. Sedov, L.I. *Similarity and Dimensional Methods in Mechanics*, 1st ed.; Academic Press: New York, NY, USA; London, UK, 1959.
26. Taylor, G.I. The formation of a blast wave by a very intense explosion. *Proc. Roy. Soc. A* **1950**, *201*, 159–174.
27. Gilev, S.D.; Anisichkin, V.F. Interaction of aluminum with detonation products. *Combust. Explos. Shock Waves* **2006**, *42*, 107–115. [CrossRef]
28. Gordon, J.M.; Gross, K.C.; Perram, G.P. Fireball and shock wave dynamics in the detonation of aluminized novel munitions. *Combust. Explos. Shock Waves* **2013**, *49*, 450–462. [CrossRef]
29. Aouad, C.J.; Chemissany, W.; Mazzali, P.; Temsah, Y.; Jahami, A. Beirut explosion: TNT equivalence from the fireball evolution in the first 170 milliseconds. *Shock Waves* **2021**, *31*, 813–827. [CrossRef]
30. Kim, H.J.; Hwang, K.; Yoon, Y.H.; Lee, H.-J. Numerical analysis of the effect of afterburning on damage to the concrete structure under interior explosion. *Int. J. Concr. Struct. Mater.* **2022**, *16*, 6. [CrossRef]